



# A potential EBV-related classifier is associated with the efficacy of immunotherapy in gastric cancer

Yun-Yun Xu, Ao Shen, Zhao-Lei Zeng

Department of Experimental Research, Sun Yat-sen University Cancer Center, State Key Laboratory of Oncology in South China, Collaborative Innovation Center for Cancer Medicine, Sun Yat-sen University, Guangzhou, China

*Contributions:* (I) Conception and design: All authors; (II) Administrative support: All authors; (III) Provision of study materials or patients: YY Xu; (IV) Collection and assembly of data: All authors; (V) Data analysis and interpretation: All authors; (VI) Manuscript writing: All authors; (VII) Final approval of manuscript: All authors.

*Correspondence to:* Zhao-Lei Zeng, MD, PhD. 651 Dongfeng Road East, Guangzhou 510060, China. Email: zengzhl@sysucc.org.cn.

**Background:** Gastric cancer (GC) is a global health problem. As a complicated heterogeneous disease, The Cancer Genome Atlas (TCGA) Research Network recognized four subtypes of GC, including Epstein-Barr virus (EBV)-positive GC (EBVaGC), which accounts for approximately 9% of all GC cases. The response to immunotherapy in GC is limited, and whether EBV status is a predictor of immunotherapy remains controversial.

**Methods:** The differential gene expression analysis was utilized to compare the gene expression between the EBV-positive group and the EBV-negative group in the TCGA-Stomach Adenocarcinoma (TCGA-STAD) cohort. Weighted gene co-expression network analysis (WGCNA), protein-protein interaction (PPI) network analysis, and gene functional enrichment analysis were used to investigate the most pivotal hub genes and their roles. The “Estimation of Stromal and Immune cells in Malignant Tumours using Expression data” (ESTIMATE) and CIBERSORT algorithms were performed to infer the immune compositions of tissue samples. Furthermore, quantitative real-time polymerase chain reaction (RT-qPCR) and survival analysis were used to validate the expression and prognosis of these hub genes in Sun Yat-sen University Cancer Center (SYSUCC) cohort. A GC cohort that received anti-programmed cell death 1 (PD-1) therapy was used to analyze the predicted efficacy based on the expression of hub genes.

**Results:** There is a total of 1,686 differentially expressed genes (DEGs) between the EBV-positive group and EBV-negative group, and WGCNA identified a yellow-colored module that was most related to EBV features. Functional enrichment analysis of 144 genes in this yellow module demonstrated that these genes primarily performed immune-related functions, and PPI network analysis through the CytoHubba plug-in identified 11 hub genes in the network. The RT-qPCR results in the SYSUCC cohort further validated that the hub genes were all increased in the EBV-positive group. Finally, we found that a potential classifier was associated with the efficacy of immunotherapy based on the expression of these 11 hub genes.

**Conclusions:** Our study identified several hub genes associated with EBV status that are closely related to the immune microenvironmental features of EBVaGC and may be used as molecular markers for predicting the immune response in GC.

**Keywords:** Gastric cancer (GC); Epstein-Barr virus (EBV); immunotherapy; hub genes

Submitted Feb 23, 2022. Accepted for publication May 17, 2022.

doi: 10.21037/tcr-22-461

View this article at: <https://dx.doi.org/10.21037/tcr-22-461>

## Introduction

Gastric cancer (GC) is a global health problem and the third leading cause of cancer death worldwide (1-3). The Cancer Genome Atlas (TCGA) Research Network recognized four distinct molecular subtypes of GC in 2014, including Epstein-Barr virus (EBV)-positive, microsatellite instable (MSI), genomically stable (GS), and chromosomal instable (CIN) GC (4). EBV-positive GC (EBVaGC) is defined by EBV infection in cancer cells, which accounts for approximately 9% of all GC cases (5,6). Compared to EBV-negative GC (EBVnGC) patients, those infected patients have a favorable survival (7,8), which suggests a unique characteristic of EBVaGC.

Therapeutic strategies for GC remain limited, and immunotherapies, such as programmed cell death 1 (PD-1) inhibitors, only benefit a few GC patients. Previous research observed dramatic responses of EBVaGC patients after immunotherapy. Several studies reported that patients with EBV-positive tumors derived longer clinical benefits with anti-programmed cell death-ligand 1 (PD-L1) antibody treatments (9-13). This beneficial effect may be associated with the active immune microenvironment induced by EBV infection. Compared to EBV-negative tumors, EBV-positive status induces a tumor microenvironment with ample immune cell infiltration and elevated expression of immune response genes (5,14-16). However, the effect of immunotherapy in EBVaGC is inconsistent, and no predictive biomarkers for effectiveness were reported (7,11,14). Therefore, it is necessary to explore EBV infection-induced changes of immune status and the tumor microenvironment and identify potential biomarkers for the selection of EBVaGC patients who might obtain greater benefits from immunotherapy.

To explain the distinct molecular features of EBV-positive status, we first employed differential gene expression analysis by comparing RNA-seq of EBVaGC patients and EBVnGC patients in the TCGA-Stomach Adenocarcinoma (TCGA-STAD) cohort and generated a co-expression network using the weighted gene co-expression network analysis (WGCNA) method. Subsequently, we further performed Gene Ontology (GO) enrichment analysis and Kyoto Encyclopedia of Genes and Genomes (KEGG) pathway analysis to investigate the functions of these differentially expressed genes (DEGs). To explore the EBV infection-induced changes in immune status, the “Estimation of Stromal and Immune cells in Malignant Tumours using Expression data” (ESTIMATE)

and CIBERSORT algorithms were used to evaluate the tumor microenvironment compositions in each tumor tissue sample. Notably, we identified a potential classifier related to the efficacy of immunotherapy. Our results suggested that this classifier may be used as a potential biomarker to identify patients with GC who are most likely to benefit from immunotherapy. We present the following article in accordance with the TRIPOD reporting checklist (available at <https://tcr.amegroups.com/article/view/10.21037/tcr-22-461/rc>).

## Methods

### *Data resources and pre-processing*

In this study, we utilized 3 different datasets for analysis. TCGA-STAD was defined as the discovery dataset, including 375 tumor samples and 32 normal samples. The RNA-seq data at the count and Fragments Per Kilobase per Million (FPKM) levels were downloaded through the “TCGAbiolinks” (17) R package. Count data were used for differential gene expression analysis through the “DESeq2” (18) R package, and the FPKM values were then transformed into Transcripts Per Kilobase Million (TPM) values for subsequent analysis. Genome annotation files were downloaded from Gencode ([http://ftp.ebi.ac.uk/pub/databases/gencode/Gencode\\_human/release\\_22/gencode.v22.annotation.gtf.gz](http://ftp.ebi.ac.uk/pub/databases/gencode/Gencode_human/release_22/gencode.v22.annotation.gtf.gz)) to transform the Ensembl ID to gene symbols and separate protein-coding genes. EBV information was obtained as described in a previous publication (19), which included 263 GC patients. We then took the intersection between 375 tumor samples and 263 samples that had EBV information and obtained a total of 228 tumor samples that contained exact EBV information (including 207 EBV-negative tumor samples and 21 EBV-positive tumor samples) for subsequent analyses.

The second dataset was from our hospital, named the Sun Yat-sen University Cancer Center (SYSUCC) cohort. A total of 137 fresh-frozen tumor tissues, including 70 archived EBV-positive GC specimens and 67 EBV-negative tissue samples, were obtained from GC patients who underwent surgical resection at SYSUCC. The clinicopathological characteristics of the patients were summarized in [Table S1](#). The Institutional Research Ethics Committee of SYSUCC approved the study.

The last dataset was a GC cohort that received anti-PD-1 therapy (11). We downloaded the transcriptome fastq files of this dataset from the European Nucleotide Archive through

accession PRJEB25780. FastQC v0.11.9 software and MultiQC v1.0.dev0 (20) software were used to examine the quality of reads, and fastp v0.23.1 (21) software was used to trim reads with low quality. STAR v2.7.9a (22) software was applied to align the reads to the human reference genome (hg38), and RSEM v1.3.3 (23) software was employed to quantify the expression of genes and transcripts.

### *Differential gene expression analysis*

TCGA-STAD RNA-seq data at the count level was applied for differential gene expression analysis by the “DESeq2” (18) R package. To identify DEGs between the EBV-positive group and EBV-negative group, we set the cutoff as  $|\log_2FC| > 1.5$  and adjusted P value  $< 0.05$ . Only genes that met this filtering criterion were considered as the DEGs, and we generated a volcano plot to visualize these DEGs using the “ggplot2” R package.

### *Weighted gene co-expression network analysis*

To investigate the relationship between the expression of DEGs and clinical EBV phenotype, we performed weighted gene co-expression network analysis through the “WGCNA” (24) R package. Firstly, the expression matrix of DEGs was set as the input file, and Pearson correlations between each gene and the other genes were calculated to generate a gene-gene correlation matrix. After that, the optimal solution of the parameter  $\beta$  of the adjacency function was determined, and the adjacency matrix was constructed to make the gene-gene correlation coefficient matrix meet the requirements of a scale-free network. Next, we constructed a topological overlap measure (TOM) matrix. In addition to simply considering the direct relationship of genes in pairs, the TOM matrix can also be more in line with the mutual effects of genes in the organism. Finally, we converted the TOM matrix to a dissimilarity matrix and used the dynamic cut tree method to perform hierarchical clustering and construct the gene modules. The minimal gene number in each module was set as 50. We correlated these gene modules with the clinical EBV feature to determine the best correlation module with the EBV phenotype.

### *Functional enrichment analysis*

GO functional enrichment analysis and KEGG pathway

analysis for genes in the selected module were performed using the “clusterProfiler” (25) R package. The function “dotplot” was used to visualize the enrichment results. An adjusted P value  $< 0.05$  was considered statistically significant.

### *Estimation of the tumor microenvironment and proportions of immune cells*

To study differences in the composition of the tumor immune microenvironment between the EBV-positive group and the EBV-negative group, we used the “Estimation of Stromal and Immune cells in Malignant Tumours using Expression data” (ESTIMATE) R package (26) and CIBERSORT (27) algorithms to evaluate the immune microenvironment of the tumor tissues. ESTIMATE calculated the stromal score, immune score, ESTIMATE score, and tumor purity. CIBERSORT was performed to evaluate the proportion of 22 different types of tumor immune infiltrating cells (TIICs) in each tumor sample. Differences in the scores and infiltrating cell proportions between the EBV-positive group and the EBV-negative group were compared by using the Wilcoxon test.

### *Protein-protein interaction (PPI) network construction and hub gene identification*

We uploaded all genes in the selected module to the STRING website (<https://string-db.org/>) to construct the PPI network. All parameters were set as default, and the generated network was exported for visualization and subsequent network-based analysis in Cytoscape v3.8.2 software (28). The CytoHubba plug-in (29) provides 12 different methods to identify the vital nodes in the PPI network. To identify the key genes with the most recognition times among these 12 methods, we first analyzed the top 10 key genes in the PPI network using the 12 methods in the CytoHubba plug-in and then counted the occurrence of these genes. Genes that occurred 5 or more times were finally identified as the hub genes.

### *Quantitative real-time polymerase chain reaction (RT-qPCR)*

Total RNA from tissues was extracted using TRIzol reagent (15596018, Invitrogen, Carlsbad, California, USA) and converted to cDNA using the Prime Script RT Master

Mix Kit (RR036A, Takara, Tokyo, Japan) according to the manufacturer's instructions. RT-qPCR analysis was performed using a LightCycler 480 instrument (Roche Diagnostics, Switzerland) by using GoTaq qPCR Master Mix (A6002, Promega, Madison, Wisconsin, USA). Relative mRNA expression was normalized to  $\beta$ -actin, and the fold change was calculated with the  $2^{-\Delta\Delta C_t}$  method. The primers used in this study were listed in [Table S2](#).

### *Survival analysis of hub genes*

We used gene expression data and survival information from the SYSUCC cohort to analyze the effect of hub genes on prognosis. Each gene was divided into two groups, high expression and low expression, according to the median value. The R packages "survival" and "survminer" were employed to plot the Kaplan-Meier survival curves and perform log-rank tests to compare the survival differences of the two groups.  $P < 0.05$  was considered statistically significant.

### *Immunotherapy efficacy analysis*

As mentioned earlier, the cohort of Kim *et al.* (11) was an anti-PD-1-treated GC cohort, and we downloaded their transcriptome data for reprocessing and quantified the expression profiles. After that, we extracted the TPM expression values of 11 key genes, used the R package "pheatmap" to plot the expression heatmap of these 11 genes, and clustered the genes according to the default parameters of the pheatmap function. According to the clustering result, we counted the number of treatment response cases and calculated the objective response rate (ORR) and clinical benefit rate (CBR) in each subclass.

### *Statistical analysis*

In addition to the results of RT-qPCR, the statistical analyses and visualization of all other data were completed using R 4.1.0 software. Statistical analyses and visualization of RT-qPCR results were performed by GraphPad Prism 7 software. All statistical methods are described in detail above.

### *Ethical statement*

The study was conducted in accordance with the Declaration of Helsinki (as revised in 2013).

## **Results**

### *The DEGs and the most relevant module to EBVaGC*

The flowchart of this study is shown in [Figure 1](#). To explore the relationship between gene expression and EBV infection phenotype, we performed a differential gene expression analysis by comparing the EBV-positive group and the EBV-negative group in the TCGA-STAD cohort, which included 207 EBV-negative and 21 EBV-positive tumor samples for subsequent analysis. As shown in [Figure 2A](#) and website: <https://cdn.amegroups.com/static/public/tcr-22-461-01.xlsx>, a total of 1,686 DEGs were obtained, including 127 upregulated DEGs and 1,559 downregulated DEGs. To investigate the relationship between the expression of DEGs and the clinical EBV phenotype, we used these DEGs to perform weighted gene co-expression network analysis using the "WGCNA" (24) R package. As shown in [Figure 2B](#), the optimal value of parameter  $\beta$  was set as 3. Subsequently, we performed the dynamic tree cut method and obtained 16 gene modules ([Figure 2C](#)). The yellow module was the most correlated module to the EBV-positive phenotype ([Figure 2D](#)), which had 144 genes, including 90 upregulated DEGs and 54 downregulated DEGs. In summary, we obtained DEGs and the most relevant module to EBVaGC by performing differential gene expression analysis and WGCNA.

### *Genes in the yellow module primarily perform immune-related functions*

To explore the function of genes in the yellow module, we performed GO enrichment analysis and KEGG pathway analysis. At the biological process level, these genes primarily regulate the activation and adhesion of immune cells, including T cell activation, regulation of cell-cell adhesion, regulation of T cell activation, calcium ion homeostasis, and regulation of leukocyte cell-cell adhesion ([Figure 3A](#)). At the molecular function level, these genes primarily regulate the activities of cytokines and chemokines, including receptor-ligand activity, signaling receptor activator activity, cytokine activity, cytokine receptor binding, and chemokine activity ([Figure 3B](#)). Furthermore, these genes were primarily located on the external side of the plasma membrane ([Figure 3C](#)) at the cell component level and primarily enriched in several pathways regulating immune factors and cells, such as cytokine-cytokine receptor interactions, natural killer cell-mediated cytotoxicity, chemokine signaling pathways and viral

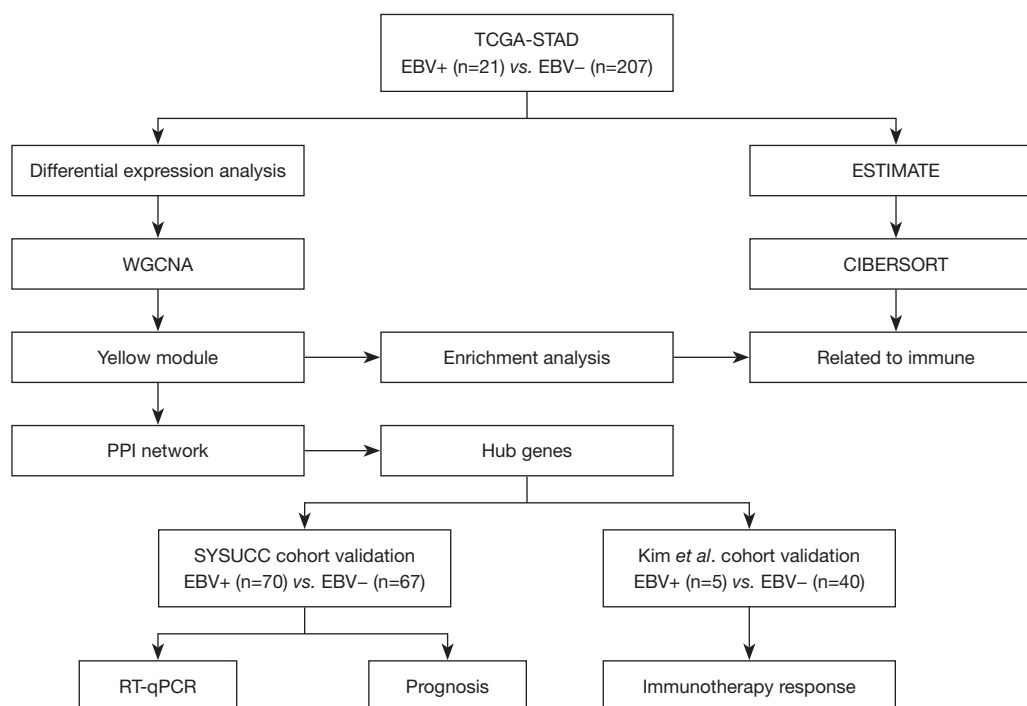


**Figure 1** The flowchart of this study. TCGA-STAD, The Cancer Genome Atlas-Stomach Adenocarcinoma; EBV, Epstein-Barr virus; WGCNA, weighted gene co-expression network analysis; PPI, protein-protein interaction; SYSUCC, Sun Yat-sen University Cancer Center; RT-qPCR, quantitative real-time polymerase chain reaction.

protein interactions with cytokines and cytokine receptors (Figure 3D). Besides, these genes were also enriched in cancer signaling pathways, such as the JAK-STAT signaling pathway (Figure 3D), which may lead to the initiation and progression of cancer. In conclusion, genes in the yellow module, which presented the characteristics of EBV status, primarily performed immune-related roles, and it may elucidate the molecular mechanisms of this special subset of EBVaGC.

#### ***Tumor microenvironment changes in the EBV-positive group***

Gene functional enrichment analysis showed that the DEGs in the EBV-positive group primarily functioned in an immune-regulating role, which prompted further exploration of the tumor microenvironment composition in tumor tissues. We first used the ESTIMATE algorithm to calculate the immune score, stromal score, ESTIMATE score, and tumor purity in each tumor tissue sample then compared these scores between the EBV-positive group and the EBV-negative group (Figure 4A-4D). We found

that the immune score and ESTIMATE score were both higher in the EBV-positive group than the EBV-negative group (Figure 4A,4B), but the stromal score between the two groups was not significantly different (Figure 4C). The tumor purity of the EBV-positive group was lower than the EBV-negative group (Figure 4D). These results suggested that the changed tumor microenvironment included more immune components in the EBV-positive group. The CIBERSORT algorithm calculates the proportion of different types of immune cells in tumor samples in more detail. Therefore, to further validate this inference, we next performed the CIBERSORT analysis to reveal the changes. As shown in Figure 4E, CIBERSORT calculated the proportions of 22 different types of immune cells and we found that CD8<sup>+</sup> T cells, M1-like macrophages, and CD4<sup>+</sup> memory-activated T cells were all elevated in the EBV-positive group. Furthermore, M0 macrophages and CD4<sup>+</sup> memory resting T cells were decreased in the EBV-positive group (Figure 4E). In summary, the components of the tumor microenvironment may be changed in EBV-positive GC, and this change might lead to an immune-activating phenotype.



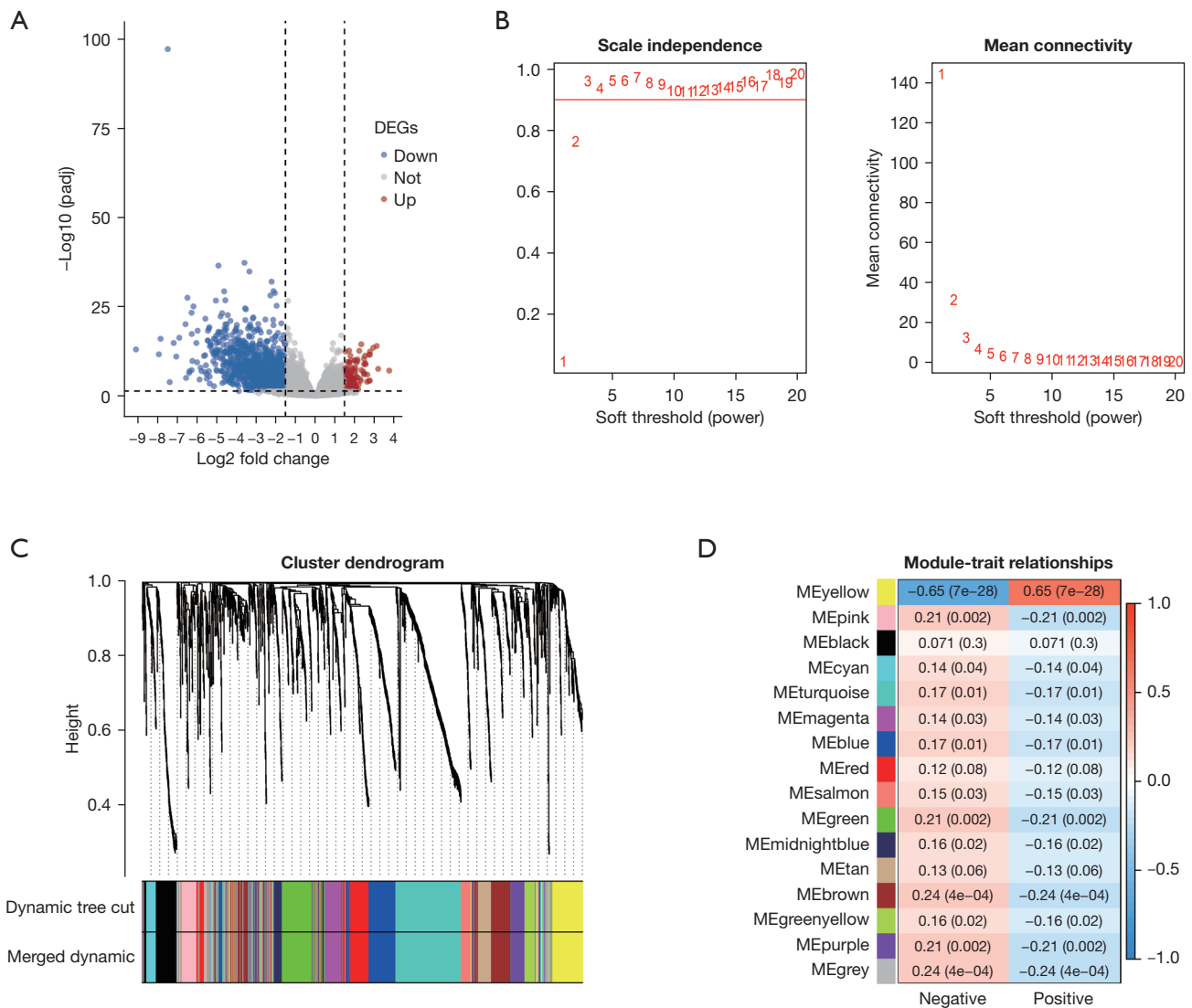


**Figure 2** Identification of the DEGs and most related modules between the EBV-positive group and EBV-negative group. (A) Volcano plot for visualizing DEGs between the EBV-positive group and EBV-negative group. The red points represent the upregulated DEGs, and the blue points represent the downregulated DEGs. (B) Topological network analysis for choosing the optimal soft threshold. (C) Dynamic tree cut after module clustering. (D) Heatmap of the correlations between multiple modules and two groups of different EBV statuses. DEG, differentially expressed gene; EBV, Epstein-Barr virus.

**Hub genes were increased in EBV-positive tumors**

There are complex interactions and connections between genes. Hub genes, which are often pivotal nodes in a PPI network, may play the most important role. The above analysis revealed a total of 144 genes in the yellow module using differential gene analysis and WGCNA. Therefore, to identify the hub genes of these 144 genes in the yellow module, we first used these genes to construct the PPI

network using the STRING website (Figure S1). Next, we counted the occurrence of the top 10 genes obtained by 12 algorithms and identified the genes with a count greater than or equal to 5 as the final hub genes (as described in the Methods and Materials section). As shown in Figure 5A and Table S3, CD8A, CXCL10, CCR5, IFNG, CXCL9, GZMA, GZMB, KLRK1, TBX21, CCL5, and CD38 were identified as the hub genes in the PPI network, which suggests that these 11 genes might have a vital function in the EBV-

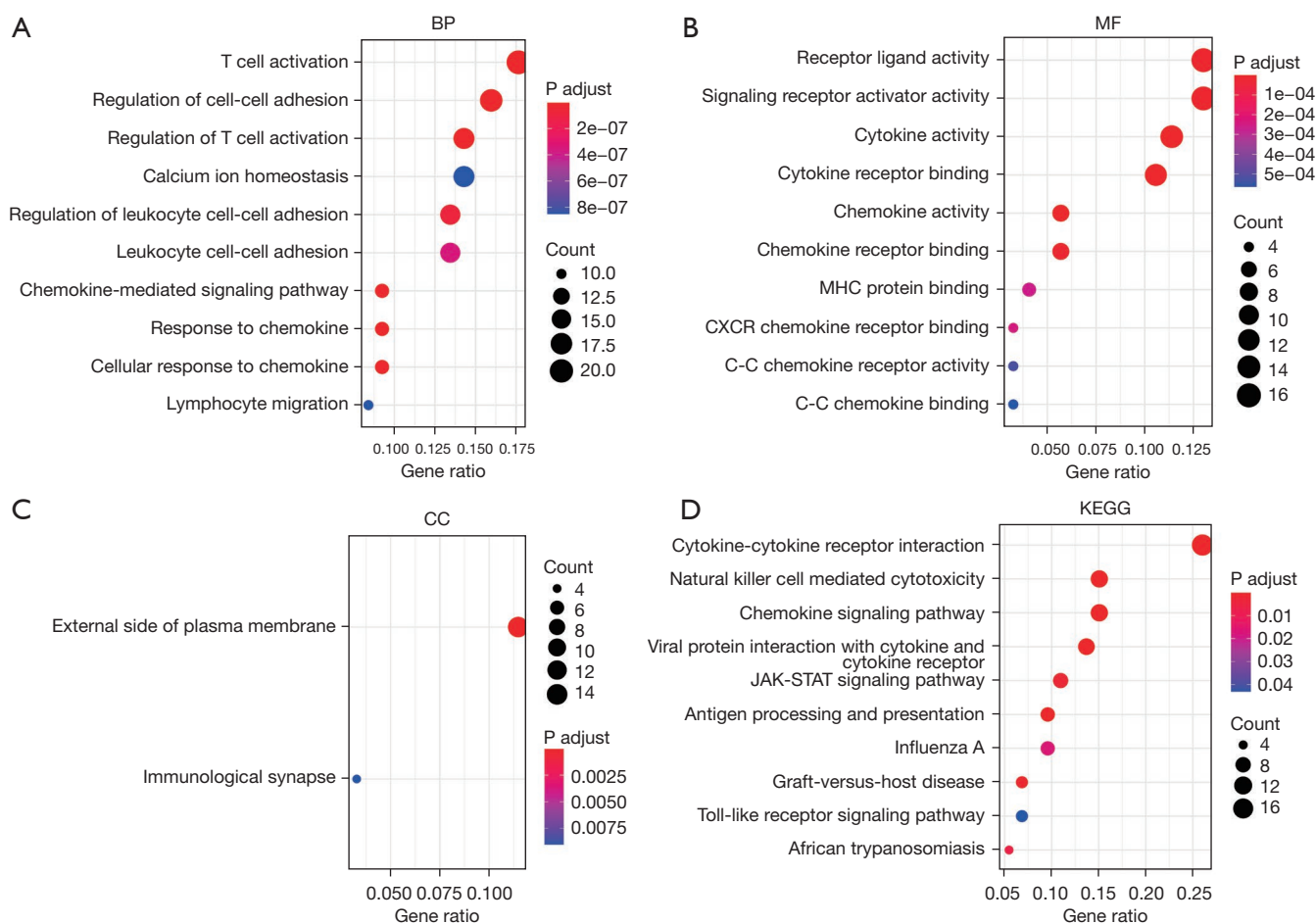


**Figure 3** Functional enrichment analysis for GO and KEGG. (A) BP; (B) MF; (C) CC; (D) KEGG. BP, biological process; MF, molecular function; CC, cellular component; GO, Gene Ontology; KEGG, Kyoto Encyclopedia of Genes and Genomes; MHC, major histocompatibility complex; CXCR, chemokine receptor; C-C, C-C motif.

positive group. Next, we used the SYSUCC cohort (including 70 EBV-positive samples and 67 EBV-negative samples) to perform RT-qPCR and validate the expression of these hub genes. *Figure 5B-5L* showed that all 11 hub genes were elevated in the EBV-positive group, which was consistent with the differential gene expression analysis (website: <https://cdn.amegroups.cn/static/public/tcr-22-461-01.xlsx>). We analyzed the prognostic role of these hub genes. As shown in *Figure S2A-S2K*, although there were no statistically significant differences in the overall survival of patients with EBV-positive GC between high and low hub gene expression, a trend of a better prognosis in patients with high expression of these genes was observed. We hypothesize that the lack of a statistically significant P value was due to the relatively small sample size. Overall,

these data suggested that several hub genes were increased in the EBV-positive group, but the prognostic roles of these genes need further validation.

#### *A potential classifier was associated with immunotherapy efficacy*

Because these hub genes were primarily immune-related, we then explored whether these genes were related to the efficacy of immunotherapy. GC has a complicated heterogeneity, and the response of EBV to immunotherapy is controversial. We investigated the role of these 11 hub genes in predicting immune efficacy in EBVaGC. To this purpose, we utilized Kim *et al.*'s cohort (11) which was a gastric cohort that received anti-PD-1 immunotherapy. The

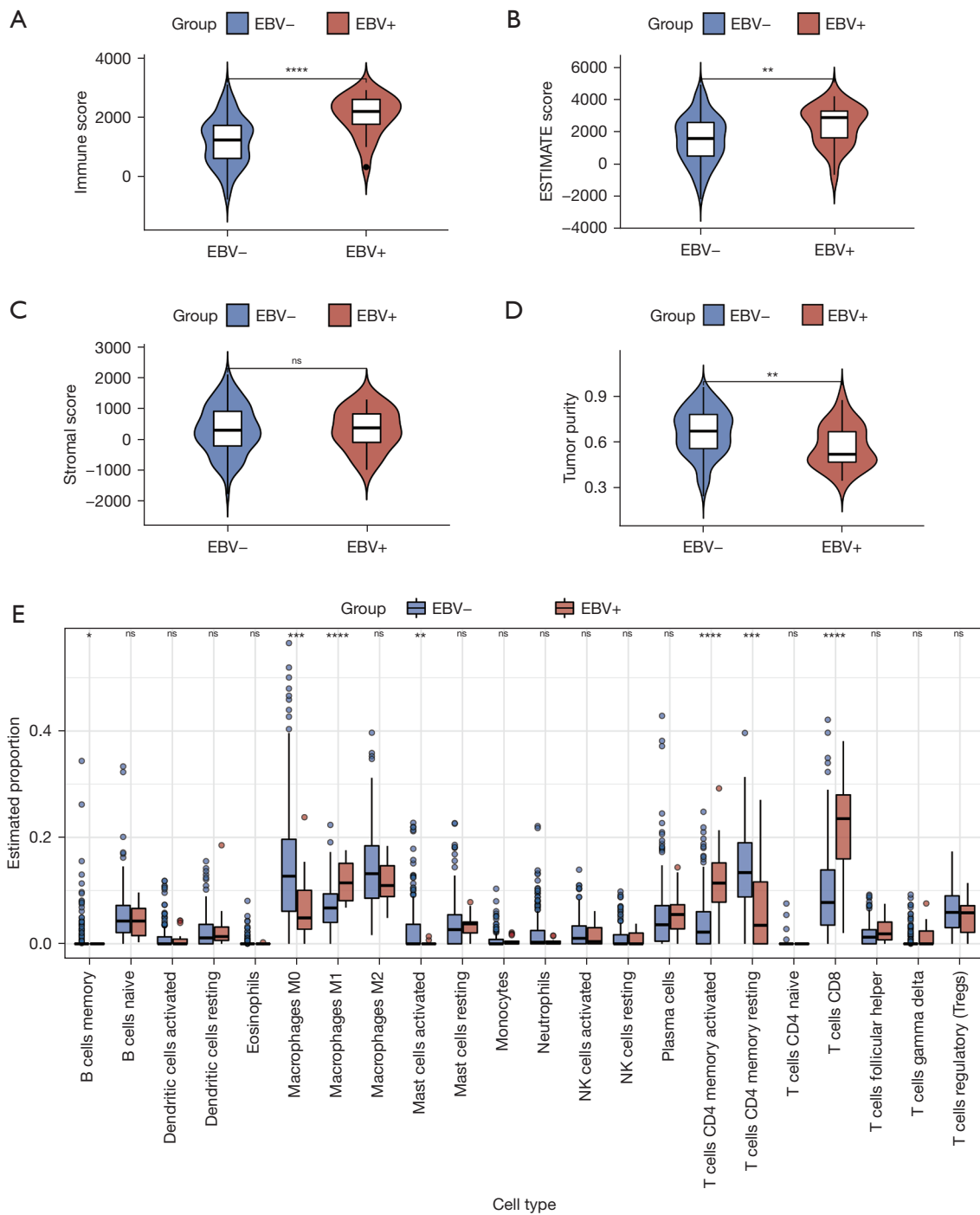


**Figure 4** Comparisons of the tumor tissue immune microenvironment between the EBV-positive group and EBV-negative group. (A) Immune score, (B) ESTIMATE score, (C) stromal score, and (D) tumor purity calculated by the ESTIMATE algorithm. (E) Comparison of the proportions of 22 different immune cells between the EBV-positive group and the EBV-negative group. \*, P<0.05; \*\*, P<0.01; \*\*\*, P<0.001; \*\*\*\*, P<0.0001; and ns means not significant. EBV, Epstein-Barr virus; NK, natural killer.



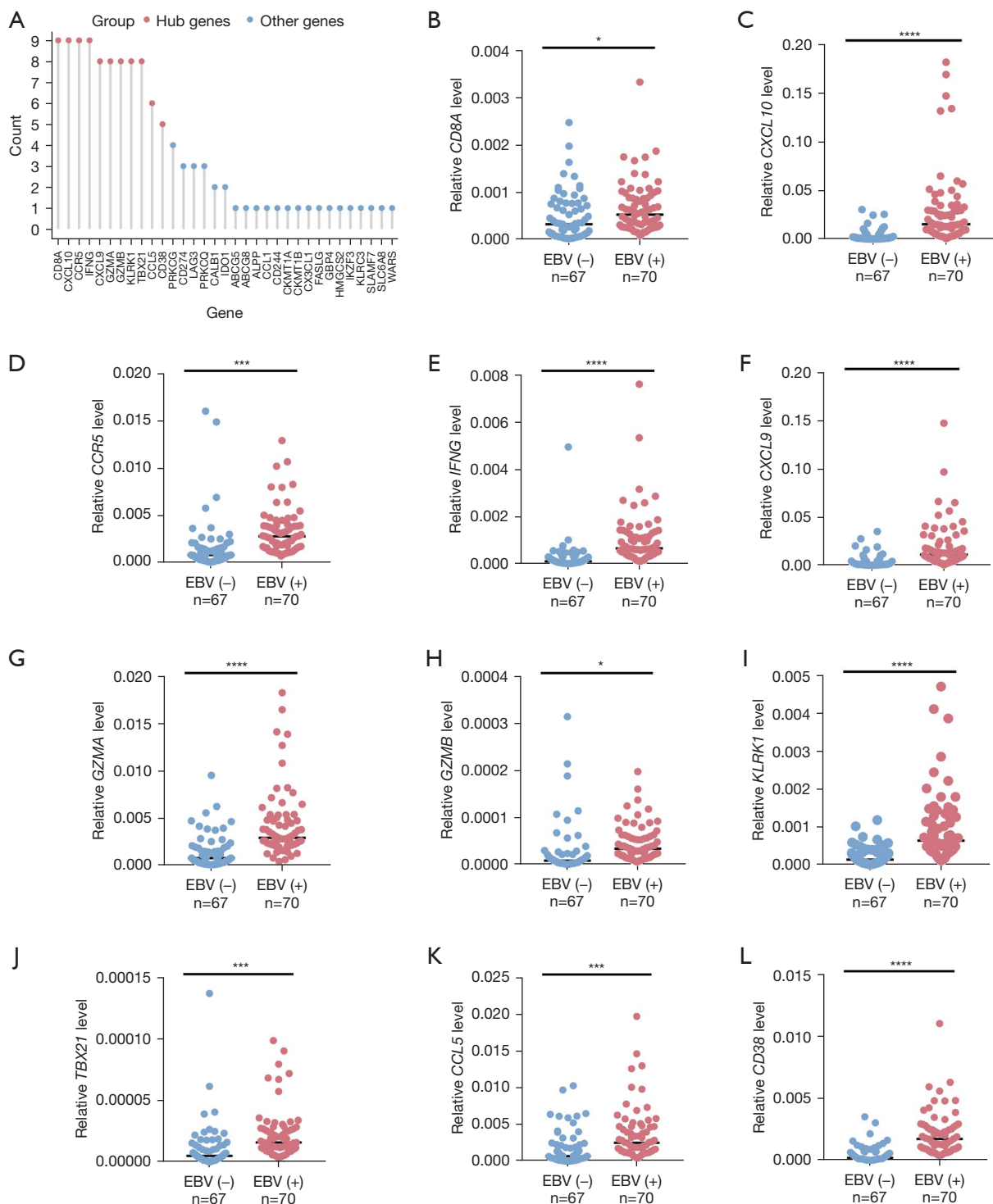


**Figure 5** Identification and validation of hub genes in the PPI network. (A) Counts of the top 10 key genes in the protein-protein interaction network analyzed using the 12 algorithms in the CytoHubba plug-in. Red points are hub genes with counts greater than or equal to 5, and blue points are genes with a count less than 5. (B-L) The expression of these 11 hub genes in the SYSUCC cohort. \*,  $P < 0.05$ ; \*\*\*,  $P < 0.001$ ; and \*\*\*\*,  $P < 0.0001$ . EBV, Epstein-Barr virus; PPI, protein-protein interaction.

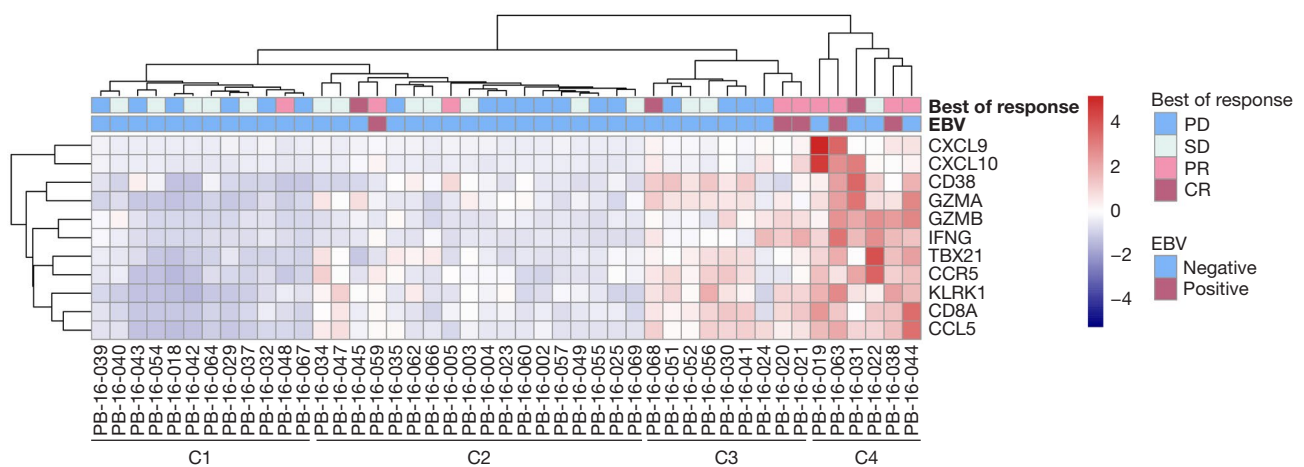


**Figure 6** A cluster heatmap of the expression of 11 genes in a cohort of gastric cancer patients receiving immunotherapy. Each row represents a gene, and each column represents a sample. Expression values in the heatmap were standardized by scale parameter. C1, cluster 1; C2, cluster 2; C3, cluster 3; C4, cluster 4. EBV, Epstein-Barr virus; PD, progressive disease; SD, stable disease; PR, partial response; CR, complete response.

**Table 1** The response evaluation criteria (RECIST) indexes in each cluster

Cluster	All (n)	PD (n)	SD (n)	PR (n)	CR (n)	ORR (%)	CBR (%)
C1	12	6	5	1	0	1/12 (8.33)	6/12 (50.00)
C2	18	8	7	2	1	3/18 (16.67)	10/18 (55.56)
C3	9	4	2	2	1	3/9 (33.33)	5/9 (55.56)
C4	6	0	1	4	1	5/6 (83.33)	6/6 (100.00)

C1, cluster 1; C2, cluster 2; C3, cluster 3; C4, cluster 4. PD, progressive disease; SD, stable disease; PR, partial response; CR, complete response; ORR, objective response rate; CBR, clinical benefit rate.

cohort contained 45 RNA-seq samples, including 5 EBV-positive samples and 40 EBV-negative samples. We classified GC into 4 clusters according to the expression of the 11 hub genes: cluster 1 (C1), cluster 2 (C2), cluster 3 (C3), and cluster 4 (C4). The expression of these 11 genes increased gradually from C1 to C4, and the different subtypes clustered according to these 11 hub genes had different responses to immunotherapy (Figure 6). Among the EBV-positive samples, we found that 4 out of 5 cases were in the C4 subtype, while 1 sample was in the C2 subtype (Figure 6). EBV-negative tumor tissues were also present across the 4 various subclasses, which suggests heterogeneity of the expression levels in different tumor tissues. We analyzed the immune efficacy of each cluster in this cohort sequentially. As shown in Table 1, the ORR of C1 was 8.33%, and the CBR was 50%. The ORR of C2 was 16.67%, and the CBR was 55.56%. The ORR of C3 was 33.33%, and the CBR

was 55.56%. The ORR of C4 was 83.33%, and the CBR was 100%. These results suggest that groups with higher expression of these 11 hub genes were more sensitive to immunotherapy, regardless of EBV status. In summary, these data demonstrated that the classifier composed of these 11 hub genes may be used to predict immunotherapeutic response in EBVaGC and the preclinical value of this classifier may be extended to all GC patients.

**Discussion**

EBVaGC was recently identified as a subtype of GC, and infected individuals are predominantly male, younger, and have better prognoses than EBVnGC patients (4,13,30). Therefore, exploring the relationship between gene expression and the EBV-infected phenotype in GC is essential to elucidate the diversity caused by EBV infection.

Here, we observed 1,686 DEGs between EBV-positive and EBV-negative patients by performing RNA-seq analysis, and the most relevant module to the EBV-positive phenotype was discovered using WGCNA. These findings may partially explain the distinct molecular characteristics of EBVaGC.

Several reports showed that EBVaGC was often accompanied by greater immune cell infiltration, such as CD8<sup>+</sup> cytotoxic T cells and mature dendritic cells, than EBVnGC. Therefore, EBVaGC is mostly associated with an immune-active tumor microenvironment (15,31). The present study observed that genes in the yellow module mostly regulated immune cells, cytokines, and chemokines. The immune score and ESTIMATE score were both elevated in the EBV-positive group compared to the EBVnGC group, but the stromal score was not significantly different. These results further demonstrated that EBV infection changed the tumor microenvironment, which was related to an immune-activating phenotype.

A previous study showed that most EBVaGC patients were resistant to current chemotherapy options (5). Considering the higher efficacy of immunotherapy in some EBV-infected individuals, there is a need to identify predictive biomarkers of patients who are sensitive to immunotherapy. Here, we used genes in the EBV-phenotype module to construct a PPI network using STRING database and identified 11 genes as the final hub genes. Then we employed RT-qPCR using RNA from tumor tissues in SYSUCC clinical cohorts to demonstrate the higher expression of these hub genes in EBVaGC.

In terms of the purpose of this study, we identified these 11 hub genes that may be used to evaluate the efficacy of immunotherapy. We can classify GC into 4 clusters according to the expression of the 11 hub genes and the expression of these 11 genes increased gradually from C1 to C4. Notably, different subtypes clustered according to these 11 hub genes had different responses to immunotherapy and individuals with elevated expression of these 11 genes were more prone to be beneficial in immunotherapy. Therefore, this classifier may be an applicable predictor for evaluating the efficacy of immune checkpoint therapy.

There are some limitations to this study. First, our research primarily analyzed tumor tissue using a series of bioinformatics-related algorithms. Although we used our hospital cohort to validate the expression of hub genes using RT-qPCR, further experimental validation studies on

the changes in the immune microenvironment are needed. Second, when using 11 hub genes for clustering, we tried to establish a signature to predict immune efficacy through various statistical methods, but we could not use these genes to establish a predictive model due to the small sample size and relatively large number of independent variables, which is also a direction for future in-depth research.

In conclusion, our study identified several hub genes associated with EBV status that are closely related to the immune microenvironmental features of EBVaGC and may be used as molecular markers for the prediction of immune response in GC. Higher expression of these genes indicated a greater benefit of immunotherapy in GC patients.

### Acknowledgments

*Funding:* This work was supported by the National Natural Science Foundation of China (No. 82072612).

### Footnote

*Reporting Checklist:* The authors have completed the TRIPOD reporting checklist. Available at <https://tcr.amegroups.com/article/view/10.21037/tcr-22-461/rc>

*Conflicts of Interest:* All authors have completed the ICMJE uniform disclosure form (available at <https://tcr.amegroups.com/article/view/10.21037/tcr-22-461/coif>). The authors have no conflicts of interest to declare.

*Ethical Statement:* The authors are accountable for all aspects of the work in ensuring that questions related to the accuracy or integrity of any part of the work are appropriately investigated and resolved. The study was conducted in accordance with the Declaration of Helsinki (as revised in 2013). The Institutional Research Ethics Committee of SYSUCC approved the study.

*Open Access Statement:* This is an Open Access article distributed in accordance with the Creative Commons Attribution-NonCommercial-NoDerivs 4.0 International License (CC BY-NC-ND 4.0), which permits the non-commercial replication and distribution of the article with the strict proviso that no changes or edits are made and the original work is properly cited (including links to both the formal publication through the relevant DOI and the license).

See: <https://creativecommons.org/licenses/by-nc-nd/4.0/>.

## References

1. Thrift AP, El-Serag HB. Burden of Gastric Cancer. *Clin Gastroenterol Hepatol* 2020;18:534-42.
2. Yusefi AR, Bagheri Lankarani K, Bastani P, et al. Risk Factors for Gastric Cancer: A Systematic Review *Asian Pac J Cancer Prev* 2018;19:591-603.
3. Johnston FM, Beckman M. Updates on Management of Gastric Cancer. *Curr Oncol Rep* 2019;21:67.
4. Cancer Genome Atlas Research Network. Comprehensive molecular characterization of gastric adenocarcinoma. *Nature* 2014;513:202-9.
5. Naseem M, Barzi A, Brezden-Masley C, et al. Outlooks on Epstein-Barr virus associated gastric cancer. *Cancer Treat Rev* 2018;66:15-22.
6. Saito M, Kono K. Landscape of EBV-positive gastric cancer. *Gastric Cancer* 2021;24:983-9.
7. Wei XL, Liu QW, Liu FR, et al. The clinicopathological significance and predictive value for immunotherapy of programmed death ligand-1 expression in Epstein-Barr virus-associated gastric cancer. *Oncoimmunology* 2021;10:1938381.
8. He CY, Qiu MZ, Yang XH, et al. Classification of gastric cancer by EBV status combined with molecular profiling predicts patient prognosis. *Clin Transl Med* 2020;10:353-62.
9. Jia X, Guo T, Li Z, et al. Clinicopathological and Immunomicroenvironment Characteristics of Epstein-Barr Virus-Associated Gastric Cancer in a Chinese Population. *Front Oncol* 2021;10:586752.
10. Panda A, Mehnert JM, Hirshfield KM, et al. Immune Activation and Benefit From Avelumab in EBV-Positive Gastric Cancer. *J Natl Cancer Inst* 2018;110:316-20.
11. Kim ST, Cristescu R, Bass AJ, et al. Comprehensive molecular characterization of clinical responses to PD-1 inhibition in metastatic gastric cancer. *Nat Med* 2018;24:1449-58.
12. Xie T, Liu Y, Zhang Z, et al. Positive Status of Epstein-Barr Virus as a Biomarker for Gastric Cancer Immunotherapy: A Prospective Observational Study. *J Immunother* 2020;43:139-44.
13. Qiu MZ, He CY, Yang DJ, et al. Observational cohort study of clinical outcome in Epstein-Barr virus associated gastric cancer patients. *Ther Adv Med Oncol* 2020;12:1758835920937434.
14. Huang B, Li Q, Geng Q, et al. ASTE1 frameshift mutation triggers the immune response in Epstein-Barr virus-associated gastric cancer. *Signal Transduct Target Ther* 2022;7:4.
15. Cho J, Kang MS, Kim KM. Epstein-Barr Virus-Associated Gastric Carcinoma and Specific Features of the Accompanying Immune Response. *J Gastric Cancer* 2016;16:1-7.
16. Sasaki S, Nishikawa J, Sakai K, et al. EBV-associated gastric cancer evades T-cell immunity by PD-1/PD-L1 interactions. *Gastric Cancer* 2019;22:486-96.
17. Colaprico A, Silva TC, Olsen C, et al. TCGAAbiolinks: an R/Bioconductor package for integrative analysis of TCGA data. *Nucleic Acids Res* 2016;44:e71.
18. Love MI, Huber W, Anders S. Moderated estimation of fold change and dispersion for RNA-seq data with DESeq2. *Genome Biol* 2014;15:550.
19. Rooney MS, Shukla SA, Wu CJ, et al. Molecular and genetic properties of tumors associated with local immune cytolytic activity. *Cell* 2015;160:48-61.
20. Ewels P, Magnusson M, Lundin S, et al. MultiQC: summarize analysis results for multiple tools and samples in a single report. *Bioinformatics* 2016;32:3047-8.
21. Chen S, Zhou Y, Chen Y, et al. fastp: an ultra-fast all-in-one FASTQ preprocessor. *Bioinformatics* 2018;34:i884-90.
22. Dobin A, Davis CA, Schlesinger F, et al. STAR: ultrafast universal RNA-seq aligner. *Bioinformatics* 2013;29:15-21.
23. Li B, Dewey CN. RSEM: accurate transcript quantification from RNA-Seq data with or without a reference genome. *BMC Bioinformatics* 2011;12:323.
24. Langfelder P, Horvath S. WGCNA: an R package for weighted correlation network analysis. *BMC Bioinformatics* 2008;9:559.
25. Wu T, Hu E, Xu S, et al. clusterProfiler 4.0: A universal enrichment tool for interpreting omics data. *Innovation (Camb)* 2021;2:100141.
26. Yoshihara K, Shahmoradgoli M, Martínez E, et al. Inferring tumour purity and stromal and immune cell admixture from expression data. *Nat Commun* 2013;4:2612.
27. Newman AM, Liu CL, Green MR, et al. Robust enumeration of cell subsets from tissue expression profiles. *Nat Methods* 2015;12:453-7.
28. Shannon P, Markiel A, Ozier O, et al. Cytoscape: a software environment for integrated models of

- biomolecular interaction networks. *Genome Res* 2003;13:2498-504.
29. Chin CH, Chen SH, Wu HH, et al. cytoHubba: identifying hub objects and sub-networks from complex interactome. *BMC Syst Biol* 2014;8 Suppl 4:S11.
30. Yang J, Liu Z, Zeng B, et al. Epstein-Barr virus-associated gastric cancer: A distinct subtype. *Cancer Lett* 2020;495:191-9.
31. Ma J, Li J, Hao Y, et al. Differentiated tumor immune microenvironment of Epstein-Barr virus-associated and negative gastric cancer: implication in prognosis and immunotherapy. *Oncotarget* 2017;8:67094-103.

**Cite this article as:** Xu YY, Shen A, Zeng ZL. A potential EBV-related classifier is associated with the efficacy of immunotherapy in gastric cancer. *Transl Cancer Res* 2022;11(7):2084-2096. doi: 10.21037/tcr-22-461



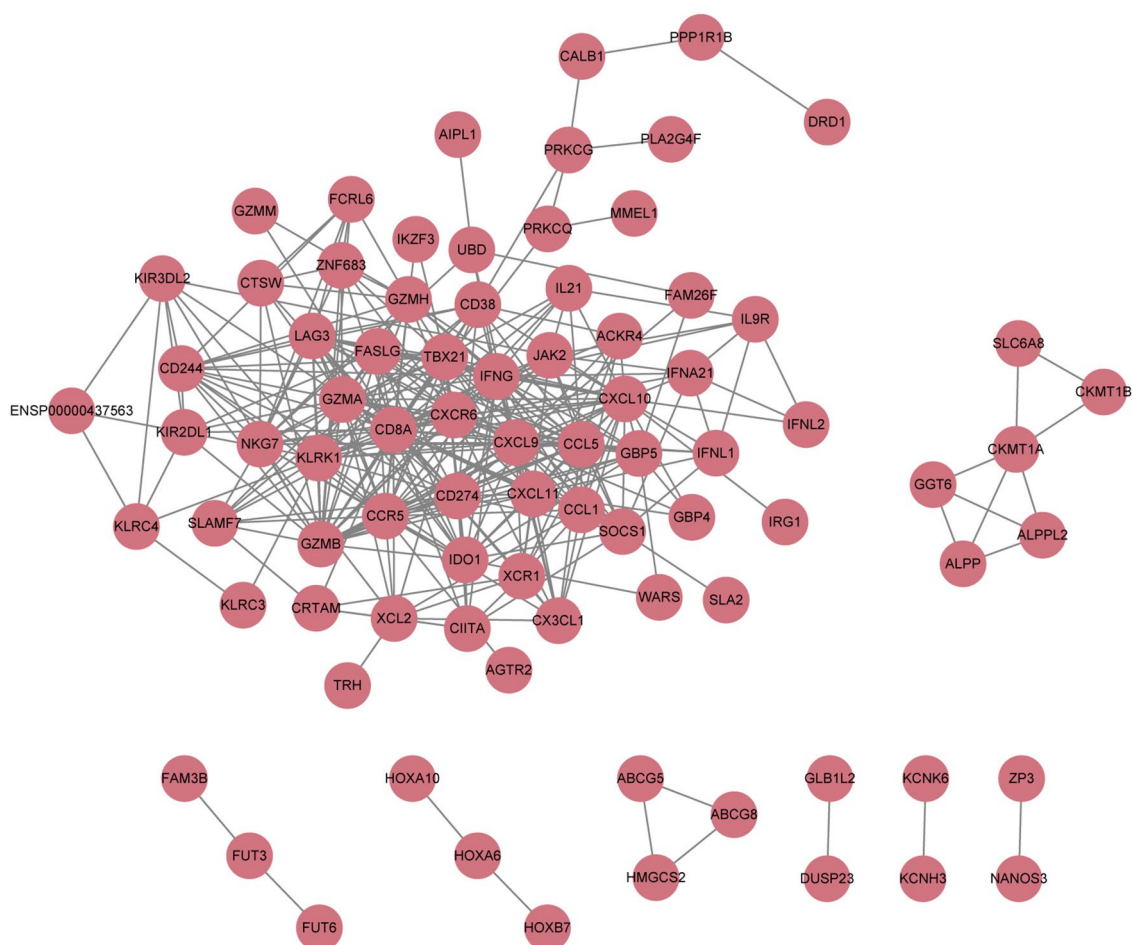


**Figure S1** The protein-protein interaction network was exported from the STRING database and visualized in Cytoscape v3.8.2 software.

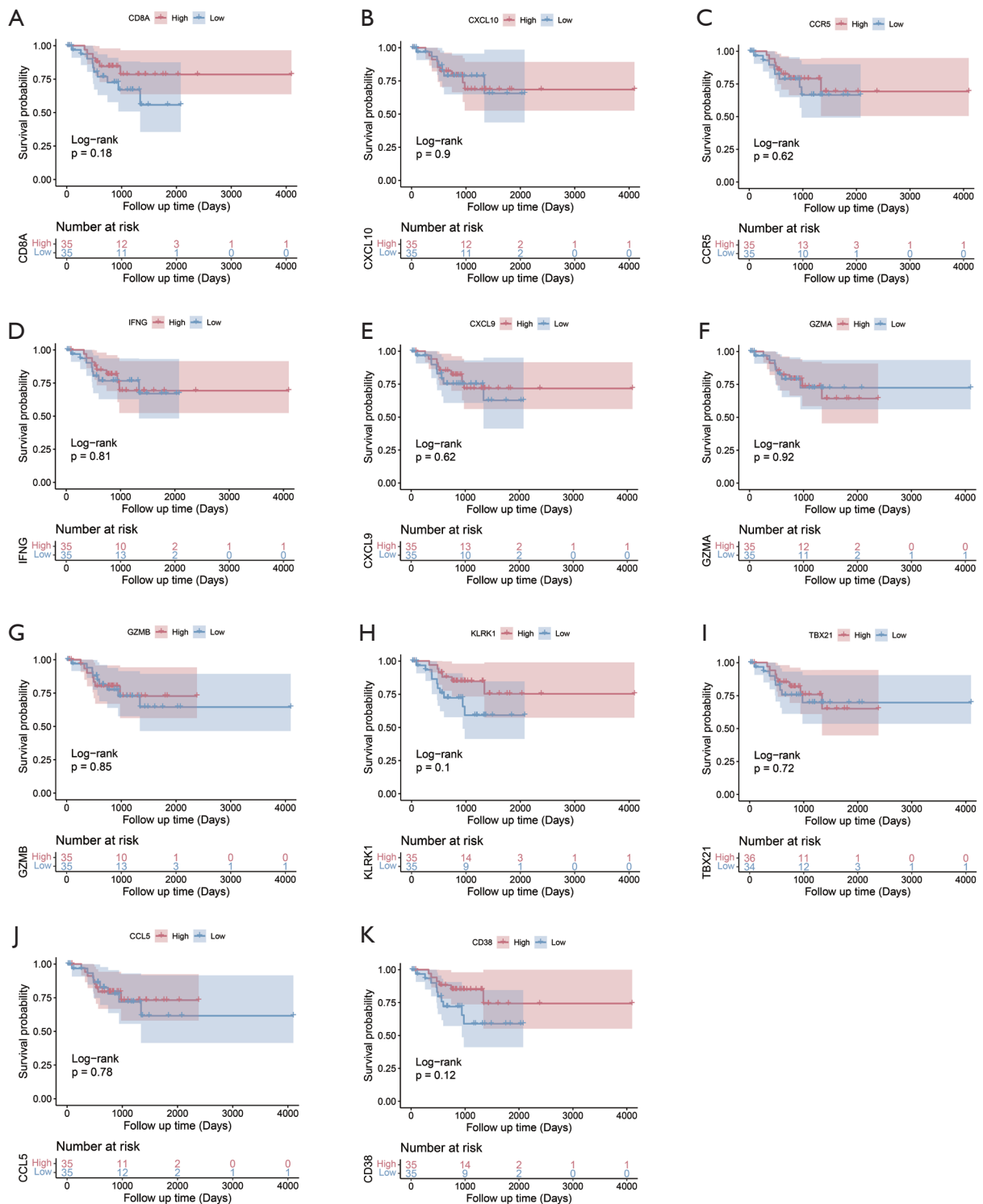


**Figure S2** Kaplan-Meier plot of 11 hub genes in the EBV-positive group of the SYSUCC cohort. The expression of each gene was divided into a high expression group and a low expression group according to its median value. The red line represents the high expression group, and the blue line represents the low expression group. (A) *CD8A*. (B) *CXCL10*. (C) *CCR5*. (D) *IFNG*. (E) *CXCL9*. (F) *GZMA*. (G) *GZMB*. (H) *KLRK1*. (I) *TBX21*. (J) *CCL5*. (K) *CD38*.

**Table S1** The clinicopathological characteristics in Sun Yat-sen University Cancer Center (SYSUCC) cohort

Variable	EBVaGC	EBVnGC	P value
Total	70	67	
Age, years			0.037
≤60	35	46	
>60	35	21	
Gender			<0.001
Male	61	39	
Female	9	28	
TNM stage			0.318
I-II	19	13	
III-IV	51	54	
Grade			<0.001
G1-G2	35	12	
G3	35	55	
Location			<0.001
Proximal	34	21	
Distal	19	39	
Whole	0	2	
Body	6	5	
Remnant	11	0	
Lauren classification			<0.001
Diffuse	6	34	
Intestine	20	17	
Mixed	43	1	
Unknown	1	15	

**Table S2** Quantitative real-time polymerase chain reaction (RT-qPCR) primers used in this study

Name	Forward Primer	Reverse Primer
$\beta$ -actin	TGGATCAGCAAGCAGGAGTA	TCGGCCACATTGTGAACTTT
CD8A	TCCTCCTATACCTCTCCCAAAC	GGAAGACCGGCACGAAGTG
IFNG	TCGGTAACTGACTTGAATGTCCA	TCGCTTCCCTGTTTTAGCTGC
CXCL10	GTGGCATTCAAGGAGTACCTC	TGATGGCCTTCGATTCTGGATT
CCR5	TTCTGGGCTCCCTACAACATT	TTGGTCCAACCTGTTAGAGCTA
GZMB	GCAGATGCAGACTTTTCCTTC	TCTCGTATCAGGAAGCCACC
CD38	AGACTGCCAAAGTGTATGGGA	GCAAGGTACGGTCTGAGTTCC
TBX21	GCCCACGATGAAACCTGAGA	GCTCCTTCATGCCCAAGACT
CCL5	TTTCTGTATGACTCCCGGC	AAGCCTCCCAAGCTAGGACA
GZMA	ATTCTTGGGGCTCACTCAATAAC	GGGTCATAGCATGGATAGGGAAA
CXCL9	ATTGGTGCCAGTTAGCCTC	CCACCGGACAGCACTCTAAA
KLRK1	CCTTGACCGAAAGTTACTGTGG	GGCTGGCATTGAGACATACAA

**Table S3** Hub gene count in CytoHubba

Gene	Count
<i>CD8A</i>	9
<i>CXCL10</i>	9
<i>CCR5</i>	9
<i>IFNG</i>	9
<i>CXCL9</i>	8
<i>GZMA</i>	8
<i>GZMB</i>	8
<i>KLRK1</i>	8
<i>TBX21</i>	8
<i>CCL5</i>	6
<i>CD38</i>	5
<i>PRKCG</i>	4
<i>CD274</i>	3
<i>LAG3</i>	3
<i>PRKCQ</i>	3
<i>CALB1</i>	2
<i>IDO1</i>	2
<i>ABCG5</i>	1
<i>ABCG8</i>	1
<i>ALPP</i>	1
<i>CCL1</i>	1
<i>CD244</i>	1
<i>CKMT1A</i>	1
<i>CKMT1B</i>	1
<i>CX3CL1</i>	1
<i>FASLG</i>	1
<i>GBP4</i>	1
<i>HMGCS2</i>	1
<i>IKZF3</i>	1
<i>KLRC3</i>	1
<i>SLAMF7</i>	1
<i>SLC6A8</i>	1
<i>WARS</i>	1